Stimulated Raman scattering with strong damping: A simple theory of the spike phenomenon

J.-G. Caputo[1,2,*] and A. Maimistov[3,†]
[1]*Laboratoire de Mathématiques, INSA de Rouen, Boîte Postal. 8, 76131 Mont-Saint-Aignan cedex, France*
[2]*Laboratoire de Physique théorique et modelisation, Université de Cergy-Pontoise and C.N.R.S., 95031 Cergy-Pontoise Cedex, France*
[3]*Department of Solid State Physics, Moscow Engineering Physics Institute, Kashirskoe sh. 31, Moscow 115409, Russia*
(Received 23 September 2004; published 8 March 2005)

The classical stimulated Raman scattering system describing the resonant interaction between two electromagnetic waves and a fast relaxing medium wave is studied by introducing a systematic perturbation approach in powers of the relaxation time. We separate amplitude and phase effects for these complex fields. The analysis of the former shows the existence of a stagnation distance after which monotonic energy transfer begins from one electromagnetic wave to the other, and this quantity is calculated. Concerning phase effects we give the conditions for the formation of a Raman spike from an initial fast and large phase jump in one of the waves. The spike evolution and width estimated from the reduced model agree with the results from numerical simulations of the original system.

DOI: 10.1103/PhysRevE.71.036601 PACS number(s): 42.25.Bs, 42.65.Dr

I. INTRODUCTION

The investigation of the transient effects in stimulated Raman scattering (SRS) has a long history. The initial interest came from the study of Druhl *et al.* [1] who examined the interaction of a strong laser pump pulse with a high-pressure gas. They found that pulses of long duration get completely depleted except in some cases where a very rapid and short-lived restoration occurs. Numerical simulations then showed that this "spike" of pump radiation was connected to a rapid π phase shift or phase flip introduced in the initial Stokes wave [2].

The theory of SRS is based on a very simple system of equations resulting from the Pluczek model of the interaction of electromagnetic waves with molecular vibrations [3,4]. This is essentially the wave equation coupled to an oscillator equation. Using a slowly varying envelope approximation for the fields and assuming the Brillouin resonance conditions on energy and momentum, one can obtain the system of a three-wave interaction between two electromagnetic waves and a medium wave (see, for example, [5]). This system is interesting for its mathematical properties and can be found in many fields. First, in the limit of zero damping Chu and Scott [6] showed that it can be written as zero-curvature conditions for two differential operators, so that an inverse scattering transform (IST) method [7] could be used to solve it. However, IST methods are generally used to solve Cauchy problems where one is given all the field data for all space coordinates at an initial time t_0. The theory of SRS leads to a boundary value problem where the fields are given for all times at a fixed location x_0. As illustrated in [8,9] the IST method can be developed in this case as well but one needs to check independently that the potential decays sufficiently fast at infinity. This approach was recently validated for the model with group velocity dispersion by direct comparison with the numerical solution of the problem [10].

From another point of view the SRS is an example in optics of the very important phenomenon of three-wave interaction. Its specificity is that two of the waves have equal velocities. A second well-known example is Mandelstam-Brillouin scattering where an optical wave interacts with acoustic phonons. As well as SRS this interaction is now used to amplify directly laser pulses propagating in an optical fiber [11–13]. Second-harmonic generation in noncollinear beams is another example of a three-wave interaction. Overall this phenomenon is present in much of condensed matter physics, from the scattering of spin waves on phonons [14] to the nonlinear optics of Bose-Einstein condensates [15,16]. Therefore the results obtained for SRS can be transposed to these other contexts.

Here we are interested in the limit where the damping of the medium vibrations is large, so that a perturbation theory derived from the IST method is not applicable. This is precisely when one observes the Raman spike, where the pump radiation after being depleted displays a sharp burst of energy, which lasts a small fraction of its initial duration. This phenomenon first observed in gases can be studied via numerical simulations of the full equations [2,17]. These show that the Raman spike can be seen only for large dissipation, that it appears with some delay, and that its amplitude decays for increasing propagation distances in the medium. Our aim is to understand how this occurs—more precisely, to (i) understand quantitatively the energy transfer from one component of the field (the pump) to the other (Stokes wave), in particular estimate the distance necessary for a given transfer, (ii) explain the time delay of the Raman spike (stagnation effect), (iii) explain the position, width, and amplitude of the Raman spike as a function of the initial phase flip in the Stokes wave, and (iv) understand the evolution of the fronts of the pump pulse.

We consider a simplified situation where the pump and Stokes pulses are not Gaussian but almost rectangular. In this case we will see that the effects of phase and amplitude can be separated so that the magnitude of the wave intensities can be assumed to be independent of time in the spike re-

*Electronic address: caputo@insa-rouen.fr
†Electronic address: maimistov@pico.mephi.ru

gion, located in the middle of the pulses. The medium variable can be expressed as an integral of the product of the amplitudes of the interacting waves. This can be expanded using as a small parameter $1/\Gamma$ where Γ is the damping of the medium variable. If we limit ourselves to the leading term in this series, we obtain the well-known equations describing SRS for continuous waves and within this approximation we find the Raman transfer coefficient. At the next order we obtain a system of equations where the evolution of the pump amplitude is independent from the one of the phase. Though it cannot take into account the phase flip effects causing the Raman spike, it should be adequate for the transient phenomena occurring on the fronts of the interacting pulses. To get coupling between the phase and amplitudes of the pulses we need to consider the third-order term in the expansion of the medium variable. In this approximation the dispersion of the response is taken into account and this causes phase variations to influence the amplitudes. Thus, we have the simplest approximate theory to describe the Raman spike phenomenon. We will show that nevertheless our analytical description of the Raman spike formation reproduces the stagnation effect and yields an approximate formula for the spike width. The comparison of our analytical results with the results of the numerical simulation shows qualitative and in some cases quantitative agreement.

The paper is organized as follows. After introducing the original model in Sec. II, we describe the approximation used and obtain the zero order (standard Raman model) in Sec. III. The front effects corresponding to the first order are described in Sec. IV. Dispersion effects corresponding to the third order are given in Sec. V and analyzed in Sec. VI. We present numerical results confirming this approach in Sec. VII and conclude in Sec. VIII.

II. ORIGINAL MODEL

The system of equations describing the nonstationary stimulated Raman scattering can be written as [18]

$$\frac{\partial a}{\partial x} = qb, \quad \frac{\partial b}{\partial x} = -q^* a, \tag{1}$$

$$\frac{\partial q}{\partial t} + \Gamma q = -gab^*, \tag{2}$$

where a,b are the amplitudes of the electromagnetic field and q is the amplitude of the medium. Γ is the damping coefficient and g is the amplification coefficient. This system of equations may be presented in a dimensionless form by rescaling a,b, $a=\tilde{a}/g^{1/2}$ and $b=\tilde{b}/g^{1/2}$.

One gets, omitting the tildes,

$$\frac{\partial a}{\partial x} = qb, \quad \frac{\partial b}{\partial x} = -q^* a, \tag{3}$$

$$\varepsilon\frac{\partial q}{\partial t} + q = -\varepsilon ab^*, \tag{4}$$

where $\varepsilon=1/\Gamma$ is a small parameter because we consider the case of a large dissipation.

The initial conditions for the system are

$$x = 0, \quad a = a_0(t), \quad b = a_0(t)\rho \exp i\phi(t),$$

where $a(t)\to 0$ for $|t|\to\infty$ and the boundary condition

$$t = -\infty, \quad q = 0,$$

where the last equation indicates that the medium is initially in the ground state. The quantity $\rho=e^{-\gamma}$ is the initial amplitude difference between a and b; in most cases, we will assume $\rho\ll 1$ and $|a|_{x=0}$ to be of order 1 so that $|a|_{x=0} \gg |b|_{x=0}$. The term $\phi(t)$ is a time dependent initial phase. In the following we will assume that a_0, γ, and ϕ are real.

Equations (3) and (4) are such that $D^2(t)\equiv|a|^2+|b|^2$ is independent of x and therefore $D^2(t)=|a|^2+|b|^2=a_0^2(t)(1+\rho^2)$. There is no symmetry in exchanging a and b. In fact the evolution of the field variable q can be written

$$\varepsilon q_{xt} + q_x = \epsilon q(|a|^2 - |b|^2).$$

Even if $|a|^2-|b|^2|_{x=0}<0$, there will be no flow of energy from b to a. Note also that an initial homogeneous phase in b plays no role in the dynamics.

We discretized Eqs. (1) and (2) in both x and t using Heun's order-2 Runge-Kutta method and advance via the following algorithm.

(i) Given $a(x,t)$ and $b(x,t)$ for a given x compute $q(x,t)$ by integrating Eq. (2) in t for the initial datum $q(x,t=0)=0$.

(ii) Advance to $a(x+dx,t)$ and $b(x+dx,t)$ for all t by integrating (1) in x.

(iii) Go to step (i) with $x=x+dx$.

The scheme is started at step (i) for $x=0$ and the quality of the computation is monitored by evaluating the relative error in $|a|^2+|b|^2$. In all the runs presented it remained smaller than 10^{-5}.

III. SYSTEMATIC APPROXIMATION: THE FIRST ORDER

The equation describing the evolution of the variable q contains the product of the amplitudes of the interacting fields. This suggests to use the variables $\sigma=ab^*$ and $n=a^*a-b^*b$, so that the principal equations take the form

$$\frac{\partial \sigma}{\partial x} = -qn, \tag{5}$$

$$\frac{\partial n}{\partial x} = 2(q\sigma^* + q^*\sigma), \tag{6}$$

$$\varepsilon\frac{\partial q}{\partial t} + q = -\varepsilon\sigma. \tag{7}$$

The formal integration in Eq. (5) leads to

$$q = -\varepsilon\left(\sigma - \varepsilon\frac{\partial \sigma}{\partial t} + \varepsilon^2\frac{\partial^2\sigma}{\partial t^2} - \varepsilon^3\frac{\partial^3\sigma}{\partial t^3} + \ldots\right), \tag{8}$$

which written as an infinite expansion is an exact solution of Eq. (4), which can be obtained by integration by parts.

In the first-order approximation, the medium variable follows instantaneously the field variables:

$$q = -\epsilon\sigma.$$

This is a well-known approximation [11] where the intensities $|a|, |b|$ can be calculated exactly. We get

$$|a|^2(x,t) = D^2(t)\frac{1}{1+\rho^2 e^{2\epsilon D^2 x}}, \tag{9}$$

$$|b|^2(x,t) = D^2(t)\frac{\rho^2 e^{2\epsilon D^2 x}}{1+\rho^2 e^{2\epsilon D^2 x}}. \tag{10}$$

Here we introduce $\rho = e^{-\gamma}$ so that the key quantity in Eqs. (9) and (10),

$$\rho^2 e^{2\epsilon D^2 x} = e^{2(\epsilon D^2 x - \gamma)}.$$

We immediately see that the distance x_c past which a significant transfer of energy occurs is

$$x_c = \frac{\gamma}{\epsilon D^2}, \tag{11}$$

which we will refer to as the stagnation distance. Note that this value is proportional to the dissipation coefficient Γ and is therefore large. We will find this quantity throughout this work.

To measure energy transfer between modes a and b, it is convenient to introduce the Raman transfer coefficient

$$R(x) = 1 - \frac{\int_{-\infty}^{+\infty} |a|^2 dt}{\int_{-\infty}^{+\infty} |a_0|^2 dt}, \tag{12}$$

such that $0 < R(x) < 1$. Initially $a = a_0$ so that $R(x=0) = 0$. As x increases a decreases so that R increases towards 1. Assuming a_0 to be a rectangular initial pulse $|a_0|^2(t) = H(t-t_1) - H(t-t_2)$ where H is the usual Heaviside function, we get $\int_{-\infty}^{+\infty} |a_0|^2 dt = t_2 - t_1$ and

$$\int_{-\infty}^{+\infty} |a|^2 dt = (t_2 - t_1)\frac{1+\rho^2}{\rho^2 e^{2(1+\rho^2)\epsilon x} + 1},$$

so that

$$R(x) = \rho^2 \frac{e^{2(1+\rho^2)\epsilon x} - 1}{\rho^2 e^{2(1+\rho^2)\epsilon x} + 1}. \tag{13}$$

In Fig. 1 we plot $|a(x,t)|^2$ as a function of time t for $x = 3$, 4, 5, 6, and 7 for both the solution of the partial differential equation system, Eqs. (3) and (4), shown as a solid line and the zero-order approximation (9) shown as a dashed line. The initial pulse is given by

$$a_0(t) = 0.5\{\tanh[(t-t_i)/w_t] - \tanh[(t-t_e)/w_t]\}, \tag{14}$$

where $t_i = 20$ and $t_e = 80$ are, respectively, the front and back ends of the pulse and the front width $w_t = 2$. The left (right) panel of Fig. 1 corresponds to $20 < t < 35$ ($70 < t < 85$). The zero-order approximation predicts correctly the field depletion in the center of the pulse but fails for the values of t corresponding to the incoming or outgoing fronts.

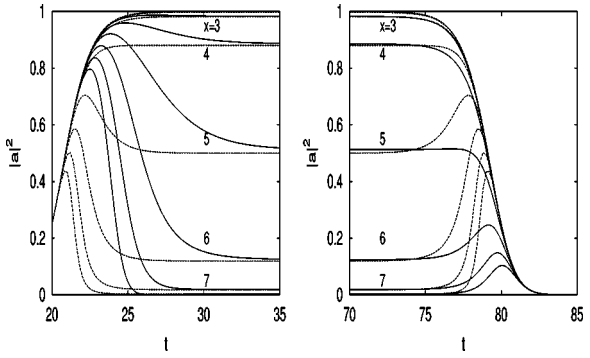

FIG. 1. Plot of $|a(x,t)|^2$ as a function of t for different values of x for the numerical solution (solid line) and the zero-order approximation (9) (dashed line). The parameter $\gamma = 5$.

Despite this disagreement on the fronts, the estimation (13) of the Raman transfer coefficient shown in Fig. 2 matches fairly well the one obtained from the full numerical solution. Since the pulse is long compared with the typical time $1/\Gamma$ (=1 here), the errors made at the front ends are compensated and the approximation is good. This would not be the case for a short pulse.

It seems clear that the transient effects occurring near an incoming or outgoing pulse cannot be captured by the zero-order approximation and that higher-order terms are needed. In the next section we include these higher-order terms, limiting ourselves to the second-order time derivative.

IV. SECOND ORDER: FRONT EFFECTS

We now consider the evolution of interacting waves up to order ε^2. We substitute the corresponding approximation for q in the initial system of equations to obtain

$$\frac{1}{\varepsilon}\frac{\partial\sigma}{\partial x} = n\left(\sigma - \varepsilon\frac{\partial\sigma}{\partial t}\right), \tag{15}$$

$$\frac{1}{\varepsilon}\frac{\partial n}{\partial x} = -2\left(2|\sigma|^2 - \varepsilon\frac{\partial|\sigma|^2}{\partial t}\right). \tag{16}$$

For simplicity, we rescale the x and t variables as $x' = \varepsilon x$ and $t' = t/\varepsilon$. We introduce the real variable p according to the

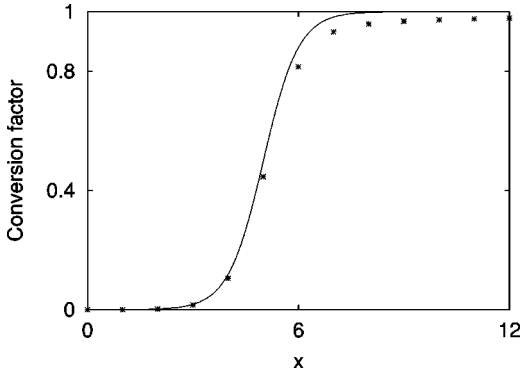

FIG. 2. Computation of the Raman transfer coefficient vs the position x for the numerical solution of Eqs. (3) and (4), shown as points and the analytical expression (13) assuming a Heaviside distribution $a_0(t)$, shown as the solid line. The parameter $\gamma = 5$.

definition $p=2\sigma\exp(-i\phi)$ so that we now only have real variables which satisfy the system of equations where we have omitted the primes:

$$\frac{\partial p}{\partial x}+n\frac{\partial p}{\partial t}=np, \tag{17}$$

$$\frac{\partial n}{\partial x}-\frac{1}{2}\frac{\partial p^2}{\partial t}=-p^2, \tag{18}$$

$$\frac{\partial \phi}{\partial x}+n\frac{\partial \phi}{\partial t}=0. \tag{19}$$

If we remember that $\sigma=ab^*$, one finds that $\phi=\arg a-\arg b$, and for $x=0$, ϕ is the function which determines the phase flip process. The system of equations given above admits the conserved quantity with respect to x:

$$p^2+n^2=D^4(t)=[a_0^2(t)+b_0^2(t)]^2. \tag{20}$$

This relation allows us to consider only two equations, one for the difference of the squares of the interacting waves and another for the phase difference ϕ:

$$\frac{\partial n}{\partial x}+n\frac{\partial n}{\partial t}=2D^3\frac{\partial D}{\partial t}+(n^2-D^4), \tag{21}$$

$$\frac{\partial \phi}{\partial x}+n\frac{\partial \phi}{\partial t}=0. \tag{22}$$

These equations agree with the initial system (5) up to order $\varepsilon^2=1/\Gamma^2$.

V. ANALYSIS OF THE CHARACTERISTIC EQUATIONS FOR AN INCOMING FRONT

We now proceed to study the effect of an incoming front using Eqs. (21) and (22). We first simplify the right-hand side of the equation for n by writing it $n^2-f(t)$ where $f(t)\equiv D^3(D-2\,\partial D/\partial t)$. Then we write the equations in characteristic form

$$\frac{dn}{dx}=n^2-f(t), \quad \frac{dt}{dx}=n. \tag{23}$$

The equation for n can be integrated using separation of variables, and we obtain

$$n=-\sqrt{f(t)}\tanh[\sqrt{f(t)}(x-x_0)] \tag{24}$$

and

$$t=t_0+\int_0^x n(\xi)d\xi=t_0-\ln\left[\frac{\cosh[\sqrt{f(t)}(x-x_0)]}{\cosh[\sqrt{f(t)}x_0]}\right], \tag{25}$$

where the square root can be imaginary so that the $i\tanh$ becomes a tan. The integration constant x_0 can be computed from the initial condition and the relation $n_0/D^2=\tanh(\gamma)$ obtained from the definition of D. We get

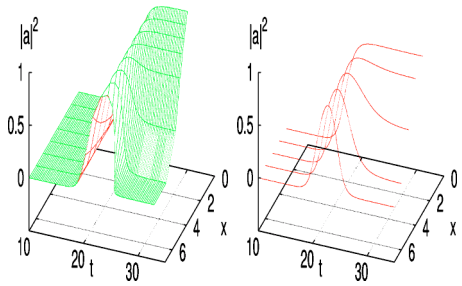

FIG. 3. Three-dimensional (3D) plot of the incoming front of Fig. 1. The left panel shows the solution obtained from the characteristics of the approximate model (23) while the right panel gives the full numerical solution of Eqs. (3) and (4).

$$x_0=\frac{1}{f}a\tanh\left[\frac{D^2}{f}\tanh(\gamma)\right].$$

Expressions (24) and (25) give n and t in implicit form and therefore need to be solved numerically.

We have integrated numerically the characteristic ordinary differential equations (23) in x and obtained the solution in the form of characteristics $t(t_0,x)$, $n(t_0,x)$. In Fig. 3 this estimation is compared to the full numerical solution of Eqs. (3) and (4) for the incoming front of Fig. 1. The results are shown in the form of 3D plots $|a(x,t)|^2$; on the left panel is the solution given by the characteristics while the full numerical solution is given in the right panel. For large x the plots on the left panel are curved because the wave breaks; i.e., it becomes multivalued. The approximate model (23) is therefore not sufficient to describe an incoming front. Second-derivative terms should be included to yield a dynamics similar to the one of Burgers equation.

VI. DISPERSION EFFECTS: THIRD-ORDER APPROXIMATION

Let us now consider terms of Eq. (8) up to third order with respect to ε. The substitution of expression

$$q=-\varepsilon\left(\sigma-\varepsilon\frac{\partial\sigma}{\partial t}+\varepsilon^2\frac{\partial^2\sigma}{\partial t^2}\right) \tag{26}$$

into the first two solutions of Eq. (5) results in the following system of equations:

$$\frac{1}{\varepsilon}\frac{\partial\sigma}{\partial x}=n\left(\sigma-\varepsilon\frac{\partial\sigma}{\partial t}+\varepsilon^2\frac{\partial^2\sigma}{\partial t^2}\right), \tag{27}$$

$$\frac{1}{\varepsilon}\frac{\partial n}{\partial x}=-2\left(2|\sigma|^2-\varepsilon\frac{\partial|\sigma|^2}{\partial t}+\varepsilon^2\frac{\partial^2|\sigma|^2}{\partial t^2}-2\varepsilon^2\left|\frac{\partial\sigma}{\partial t}\right|^2\right). \tag{28}$$

Both these equations and the original system of equations (5) have the first integral with respect to $xn^2+4\sigma^*\sigma=\text{const}(t)$.

Again we rescale x and t as as $x'=\varepsilon x$ and $t'=t/\varepsilon$ and introduce the real variable p according to the definition $2\sigma=p\exp(i\phi)$. Using the system of equations (26) and (28) one gets the following system of equations for the real variables

p, n, and ϕ where the primes have been omitted:

$$\frac{\partial p}{\partial x}+n\frac{\partial p}{\partial t}-n\frac{\partial^2 p}{\partial t^2}=np\left[1-\left(\frac{\partial\phi}{\partial t}\right)^2\right], \tag{29}$$

$$\frac{\partial n}{\partial x}-p\frac{\partial p}{\partial t}=-p^2\left[1-\left(\frac{\partial\phi}{\partial t}\right)^2\right]-p\frac{\partial^2 p}{\partial t^2}, \tag{30}$$

$$\frac{\partial\phi}{\partial x}+n\frac{\partial\phi}{\partial t}-n\frac{\partial^2\phi}{\partial t^2}=2\frac{\partial\phi}{\partial t}\left(\frac{\partial \log p}{\partial t}\right)n, \tag{31}$$

where again the conservation law (20) holds.

Since we want to take into account only effects resulting from the phase-flip process, we will neglect the terms $\partial\ln(p)/\partial t$ and $\partial^2 p/\partial t^2$. Furthermore, we will assume that D does not vary with time; i.e., we place ourselves in the central part of the rectangularlike initial pulse. Using these approximations the system of equations (29)–(31) takes the form

$$\frac{\partial n}{\partial x}+n\frac{\partial n}{\partial t}=(n^2-D^4)\left[1-\left(\frac{\partial\phi}{\partial t}\right)^2\right], \tag{32}$$

$$\frac{\partial\phi}{\partial x}+n\frac{\partial\phi}{\partial t}=0. \tag{33}$$

These equations can be written in the characteristic form [19]

$$\frac{dt}{dx}=n,\quad \frac{d\phi}{dx}=0, \tag{34}$$

$$\frac{dn}{dx}=(n^2-D^4)\left[1-\left(\frac{\partial\phi}{\partial t}\right)^2\right]. \tag{35}$$

From Eqs. (34) it follows that $\phi=\phi(t_0)$ and the expression to find characteristics,

$$t=t_0+\int_0^x n(\xi)d\xi, \tag{36}$$

where ξ is the variable of the characteristic. From Eq. (35) we can compute $n(\xi)$ as

$$n(x,t_0)=-D^2\tanh\{D^2 f(t_0)[x-x_0(t_0)]\}, \tag{37}$$

where $x_0(t_0)$ is a constant of integration and the function $f(t_0)$ is defined by

$$f(t_0)=1-\left(\frac{\partial\phi}{\partial t}\right)^2,$$

where the derivative with respect to t is calculated at $t=t_0$, and as $\phi=\phi(t_0)=\phi(x=0,t_0)$, its value can be calculated at $x=0$. Thus the function $f(t_0)$ reflects the phase flip on the initial pulse b of the interacting waves. The constant of integration $x_0(t_0)$ is defined by the initial condition

$$n(x=0,t_0)=n_0=D^2\tanh\{D^2 f(t_0)x_0(t_0)\}. \tag{38}$$

If we use Eq. (38) and the definitions of n and D, we obtain

$$n_0=a_0^2[1-\exp(-2\gamma)],\quad D^2=a_0^2[1+\exp(-2\gamma)];$$

then, the constant of integration $x_0(t_0)$ can be rewritten as $x_0(t_0)=\gamma[D^2 f(t_0)]^{-1}$. Substituting this expression into Eq. (37) leads to

$$n(x,t_0)=-D^2\tanh\{D^2 f(t_0)x-\gamma\}. \tag{39}$$

So Eqs. (36) and (39) allow us to write the expression defining the characteristics:

$$t=t_0-\frac{1}{f(t_0)}\log\left\{\frac{\cosh[\gamma-D^2 f(t_0)x]}{\cosh\gamma}\right\}. \tag{40}$$

From this equation one can extract t_0 as a function of t and x and substitute it into Eq. (39) to yield the solution of the problem under consideration:

$$n(x,t)=-D^2\tanh\{D^2 f(t_0(t,x))x-\gamma\}, \tag{41}$$

$$a^2(x,t)=0.5D^2[1-\tanh\{D^2 f(t_0(t,x))x-\gamma\}]. \tag{42}$$

There is an intrinsic difficulty in this procedure due to the fact that the characteristics can cross so that there might not be a unique t_0 for a given t and x. In particular we will see that around the spike region characteristics will cross. Nevertheless, it is possible to understand what is going on by using asympotics in the regions away from where the characteristics cross. We do this in the next section.

VII. ANALYSIS OF THE CHARACTERISTIC EQUATIONS FOR THE RAMAN SPIKE

As shown by expressions (40) and (42) the principal problem is to determine the auxiliary function $t_0(t,x)$, from the equation of characteristics, Eq. (40). To do it we will use the numerical solution of this equation. However, it is possible to obtain some information for small or large x using asymptotic expansions of the function $t_0(t,x)$. We write

$$t=t_0+\frac{1}{f}\ln[\cosh(D^2 fx)]+\frac{1}{f}\ln[1-\tanh(D^2 fx)\tanh(\gamma)]. \tag{43}$$

For x small the above expression can be expanded to yield, at first order,

$$t\approx t_0+D^2 x\tanh(\gamma)=t_0+n_0 x. \tag{44}$$

This expression can be immediately deduced from the characteristic equation giving dt/dx, Eq. (36). It is correct even in the spike region as long as $D^2 fx\ll 1$. For larger values of x it is necessary to distinguish the region where $f\ll 0$, leading to a spike from the rest of the domain where $f\approx 1$.

Let us consider this case first. Then one can approximate the expression (43) for large $x\approx 2\gamma/D^2$ by

$$t=t_0+2\gamma\tanh(\gamma)-D^2 x\tanh(\gamma). \tag{45}$$

Notice how the slope of the $t(x)$ curve—i.e., the direction of the characteristic—changes as one crosses the stagnation distance $x_c=\gamma/D^2$.

The situation in the spike region can be analyzed using the expression for n, Eq. (41). Inside the spike region the

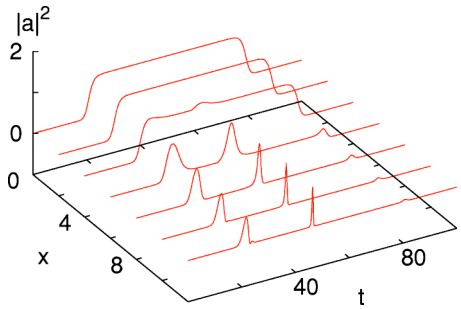

FIG. 4. 3D plot of the pump amplitude $|a|^2(x,t)$ obtained by direct integration of the original equations (3) and (4). The initial phase flip is for $t=t_f=40$ and the parameters are $\gamma=5$ and $\delta=0.011$.

argument of the tanh in n, $D^2f(t_0(t,x))x-\gamma<0$, even for large values of x so that there is no depletion. In this region the characteristics follow $t=t_0+D^2x\approx t_0+n_0x$ which is very close to Eq. (44) for large γ. On the sides of the spike $0<f<1$ so that the argument of the tanh can go through 0 but for a larger stagnation distance than x_c. To summarize, outside the spike region we expect the characteristic curves to bend smoothly from the behavior (44) to (45) as x increases while inside the spike region they will follow Eq. (44). There is also an intermediate region around the spike where the characteristic curves will shift to Eq. (45) but for $x>x_c$. These sets of characteristic curves will cross as we will show in the next section, leading to shock formation.

To understand things quantitatively let us now give a precise form of the phase-flip function. We chose

$$\phi(x=0,t)=-\frac{a_f}{2}\left[1+\tanh\left(\frac{t-t_f}{\delta}\right)\right],$$

where t_f is the location of the phase jump and a_f its amplitude. When $a_f=\pi$ we speak of phase flip. With this choice the function $f(t_0)$ takes the form

$$f(t_0)=1-\frac{a_f^2}{4\delta^2}\mathrm{sech}^4\left(\frac{t_0-t_f}{\delta}\right). \tag{46}$$

The region where the function $f(t_0)$ has a minimum will be named the *Raman spike* (RS) *region*. If the parameter δ is chosen to be small, the RS region is very narrow. Outside this region $f(t_0)$ is equal to 1. Hence we can write

$$a^2(x,t)=0.5D^2[1-\tanh(D^2x-\gamma)]. \tag{47}$$

It shows that up to $x\approx(\gamma-1)/D^2$ the value of the intensity of the pump wave is $a^2(x,t)=D^2$ and that for $x=x_c\approx\gamma/D^2$ this value decreases down to $0.5D^2$. Only inside the RS region does the intensity of the pump wave not vary. This results in the formation of a Raman spike. Figure 4 shows a 3D plot of the pump field $|a(x,t)|^2$ solution of the original equations (3) and (4) where we chose the Heaviside-like initial pump and Stokes distribution (14). In this case the middle of the pulse is such that $D=1$. We took $\gamma=5$ and clearly see in Fig. 2 that the pump field starts getting depleted only past $x_c=5$. Thus our estimation of the stagnation distance is a good one.

Let Δ_{RS} be the width of the RS pulse given by half of the amplitude—i.e., $\Delta_{RS}=2(t_1-t_m)$, where the instant t_1 is defined by the condition $a^2(x,t_1)=0.5D^2$ and t_m is the position of the minimum of the function $f(t_0)$. Using Eqs. (42) and (46) we can obtain the equation

$$\frac{a_f^2}{4\delta^2}\mathrm{sech}^4\left(\frac{t_0(t_1,x)-t_f}{\delta}\right)=1-\frac{\gamma}{D^2x}=1-\frac{x_c}{x}. \tag{48}$$

Note how the stagnation distance x_c appears again. Furthermore, if $x\leqslant x_c$, the right-hand side is negative so that no value of t_0 can be found and there is no Raman spike formation. Hence we obtain the stunted growth (stagnation) of Raman transformation once again. From the definition of the stagnation distance x_c one can see that in dimensional variables x_c is proportional to the damping coefficient Γ and to the initial depletion coefficient γ.

Let us now proceed to further analyze Eq. (48) in order to estimate the width of the Raman spike. For that denote

$$\epsilon_1^4\equiv\frac{4\delta^2}{a_f^2}\left(1-\frac{x_c}{x}\right),$$

so that Eq. (48) can be written as

$$\cosh\left(\frac{t_0(t_1,x)-t_f}{\delta}\right)=\epsilon_1^{-1}. \tag{49}$$

Since the parameter ϵ_1 is very small because of the smallness of δ, the argument of the cosh function in Eq. (49) is large so that the function can be approximated by an exponential. We obtain

$$\exp\left(\frac{t_0(t_1,x)-t_f}{\delta}\right)=\frac{2}{\epsilon_1},$$

so that $t_0(t_1,x)=t_f+\delta\ln(2/\epsilon_1)$. If the function $t_0(t,x)$ can be approximated by $t_0\approx t-n_0x$, then $t_1=t_f+n_0x+\delta\ln(2/\epsilon_1)$. But in the framework of the approximation under consideration $t_m=t_f+n_0x$, and hence $\Delta_{RS}\approx2\delta\ln(2/\epsilon_1)$. From this expression and the definition of the parameter ϵ_1 one gets

$$\Delta_{RS}\approx-\frac{\delta}{2}\ln\left[\frac{\delta^2}{4a_f^2}\left(1-\frac{x_c}{x}\right)\right], \tag{50}$$

where it was assumed that $\delta^2(x-x_c)\ll x_c$; i.e., the distance away from x_c is small large enough. It is interesting that for $x\to\infty$ the width of RS pulse approaches the limiting value

$$\Delta_{RS}\approx\delta\ln(2a_f/\delta).$$

For $\delta=0.5$ this limit is equal to 1.27. When the distance x approaches the stagnation distance x_c, the width of the RS pulse increases. Hence the Raman spike forms only if $x>x_c$, a feature that we can clearly see in Fig. 4.

VIII. NUMERICAL RESULTS AND DISCUSSION

We present here numerical solutions of the full SRS equations for the spike which confirm the analysis done previously. Equations (1) and (2) have been integrated using the method indicated in Sec. II. We first examine the influence of

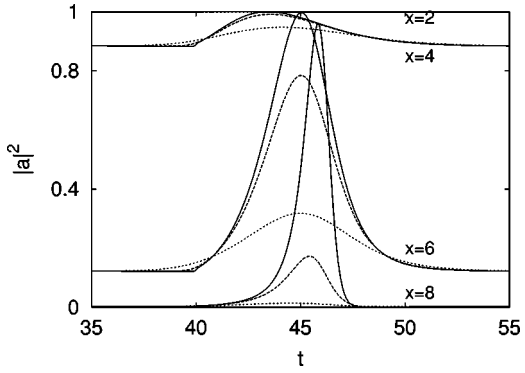

FIG. 5. Influence of flip time on the formation of the Raman spike. $|a|^2(x,t)$ for $x=2$, 4, 6, and 8 as a function of t for three different flip times $\delta=0.1$ (solid line), 1 (medium dashed line), and 3 (short dashed line). The amplitude of the flip is π and the other parameters are as in Fig. 4.

the flip time and amplitude on the formation of the spike.

Figure 5 shows $|a(x,t)|^2$ as a function of t for $x=2$, 4, 6, and 8 with a Raman spike. The calculation has been done for a flip amplitude $a_f=\pi$ and three values of flip time $\delta=0.1$ (solid line), 1 (medium dashed line), and 3 (short dashed line). As expected from the previous section, no manifestation of the phase flip can be seen for $x<x_c=\gamma/D^2\approx 4$, where x_c is the stagnation distance. Notice how the amplitude of the spike remains of order 1 for the fast flip $\delta=0.1$. On the contrary for $\delta=1$ the amplitude decays as x increases to 4 and 6. The decay is even stronger for $\delta=3$ for which the spike is barely noticeable.

The influence of the phase change on the Raman spike can be seen in Fig. 6. There we computed $|a(x,t)|^2$ as previously but took $\delta=1$ fixed and took three values of the phase jump $a_f=\pi$, $\pi/2$, and $\pi/4$. The results are similar to the ones shown in Fig. 5. No spike can be seen for $x<x_c$ and the spike dies off for $\delta=\pi/4$ whereas it is still weakly present for $\delta=\pi/2$.

These two figures show the importance of the ratio a_f/δ. If $a_f/\delta>\pi$, a Raman spike is created and subsists for a few stagnation distances. On the contrary, if $a_f/\delta<\pi$, the spike is weak and short lived.

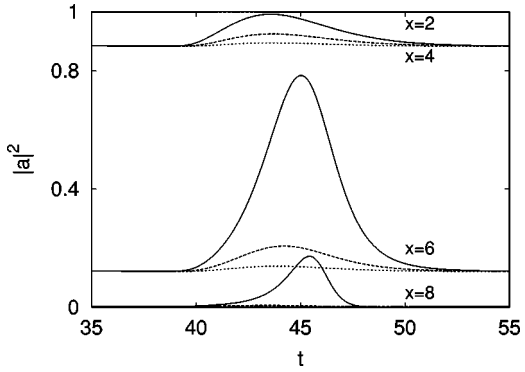

FIG. 6. Influence of the amplitude of the phase change on the formation of the Raman spike. $|a|^2(x,t)$ for $x=2$, 4, 6, and 8 as a function of t for three different phase changes of π (solid line), $\pi/2$ (medium dashed line), and $\pi/4$ (short dashed line) occurring during a time $\delta=1$.

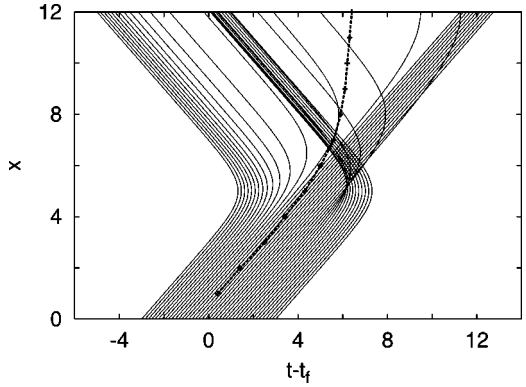

FIG. 7. Characteristic curves $t(x)$ for different values of t_0 (solid line). The parameters are the same as for Fig. 4. The dashed line indicates the position of the maximum of the spike in the numerical solution of the full system.

We now compare the position and half width of the Raman spike obtained from the direct solution of Eqs. (1) and (2) and the estimates given by the characteristic equations. Figure 7 shows the characteristic curves $t(x)$ for different values of t_0 around the spike instant $t_0=t_f$. As expected from the analysis of the previous section, one sees the characteristic curves away from the spike region shift smoothly from the behavior (44) to (45) as $x>x_c$. In the spike region the characteristics are straight and around the spike one can see the transition from (44) to (45) for a stagnation distance larger than x_c. Observe how the characteristics cross for $x>x_c$ indicating a shock. In fact there are multiple shocks as shown by the crossings seen for the curves such that $t_0\leqslant t_f$ in the right top part of the graph. For $t_0>t_f$ all the curves seem to accumulate along a line parallel to Eq. (45). This set of curves shows the limitation of the our approach which can predict the kinematics of the Raman spike as it is created,

$$n=-D^2\tanh[D^2 f(t-D^2 x\tanh(\gamma))x-\gamma], \qquad (51)$$

but breaks down after shocks are formed. In Fig. 7 we plot the maximum of the spike observed in the numerical solution of Eqs. (1) and (2) and one can see that this position agrees well with the one given by the accumulation point of the characteristics for $t_0>t_f$. The result is clearly seen in Fig. 8

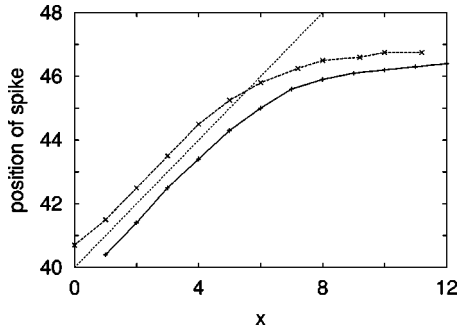

FIG. 8. Time position of the maximum of the Raman spike corresponding to Fig. 4 as a function of x (solid line). The t position where the phase of q is equal to $-\pi/2$ is given by the dashed line. The line $t=t_f+x$ is given by the short dashed line.

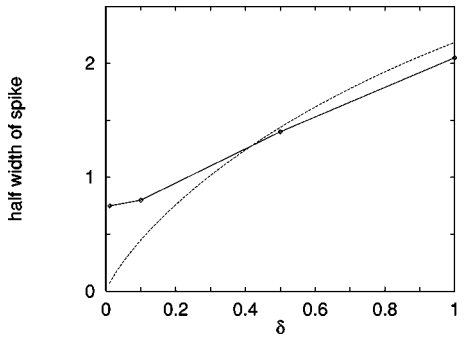

FIG. 9. Half-width of the Raman spike as a function of δ, the flip time for the numerical solution of the full system (solid line), for a distance $x=2$. $x_c=2\gamma/D^2=10$. The analytical expression (50) is given as the dashed line. The other parameters are the same as for Fig. 4.

where we plot the position of the maximum of the spike as a function of x. On the same picture we give the t^* value such that $q(x,t^*)=\pi/2$ and this follows the position of the spike. In Fig. 9 we compare the width of the Raman spike with expression (50) for a range of values of δ and see that there is a fairly good agreement.

IX. CONCLUSION

We have introduced a systematic approximation procedure to simplify the stimulated Raman scattering equations where the small parameter is the inverse of the damping of the field variable. Since the equations describe complex fields, we have studied separately the influence of the amplitude and phase of the waves. This provided a better understanding of the phenomenon.

Concerning the amplitude, the zero order of the approximation yields the well-known theory for continuous waves. At first order we obtain a hyperbolic system of equations which exhibits wave breaking. At this stage it does not give accurate front dynamics but it could probably be refined to do so. The simple model we introduce allows one to understand how energy transfer occurs between the different components a and b of the field. In particular we show that this transfer is monotonous and occurs after a stagnation distance x_c which we specifically compute from the parameters of the model.

For the phase effects we provide a good description of the Raman spike phenomenon in the case of waves of constant amplitude through a simple system of hyperbolic partial differential equations for the population difference $n=|a|^2-|b|^2$ and the relative phase of the fields. We show that a spike is formed from an initial phase jump of amplitude a_f and duration δ in one of the fields if the ratio a_f/δ is large enough. From the characteristic curves of the system we obtain the time instant and duration of the Raman spike as a function of the propagation distance in the medium. These estimations are confirmed numerically.

ACKNOWLEDGMENT

J.G.C. thanks Jerome Leon for useful discussions. The computations were done at the Centre de Resources Informatiques de Haute-Normandie.

[1] K. Drühl, R. G. Wenzel, and J. L. Carlsten, Phys. Rev. Lett. **51**, 1171 (1983).
[2] R. G. Wenzel, J. L. Carlsten, and K. Drühl, J. Stat. Phys. **39**, 621 (1985).
[3] A. Yariv, *Quantum Electronics* (Wiley, New York, 1967).
[4] R. H. Pantel and H. E. Putkhof, *Fundamentals of Quantum Electronics* (Wiley, New York, 1969).
[5] C. Claude, F. Ginovart, and J. Leon, Phys. Rev. A **52**, 767 (1995).
[6] F. Y. F. Chu and A. C. Scott, Phys. Rev. A **12**, 2060 (1975).
[7] M. J. Ablowitz and H. Segur, *Solitons and the Inverse Scattering Transform* (SIAM, Philadelphia, 1981).
[8] J. Leon, Phys. Lett. A **170**, 283 (1992); Phys. Rev. A **47**, 3264 (1993).
[9] J. Leon and A. Mikhailov, Phys. Lett. A **253**, 33 (1999).
[10] M. Boiti, J. G. Caputo, J. Leon, and F. Pempinelli, Inverse Probl. **16**, 303 (2000).
[11] G. P. Agrawal, *Nonlinear Fiber Optics* (Academic Press, San Diego, 1995).
[12] R. W. Boyd, *Nonlinear Optics* (Academic Press, London, 1992).
[13] Jake Bromage, J. Lightwave Technol. **22**, 79 (2004).
[14] G. A. Melkov, A. A. Serga, V. S. Tiberkevich, A. N. Oliynyk, and A. N. Slavin, Phys. Rev. Lett. **84**, 3438 (2000).
[15] G. Lenz, P. Meystre, and E. M. Wright, Phys. Rev. Lett. **71**, 3271 (1993).
[16] J. Javanainen and M. Mackie, Phys. Rev. A **59**, R3186 (1999).
[17] J. G. Caputo, in *Nonlinearity and Disorder: Theory and Applications*, edited by F. Kh. Abdullaev, M. P. Soerensen, and O. Bang (Kluwer, Dordrecht, 2001).
[18] A. C. Newell and J. V. Moloney, *Nonlinear Optics* (Addison-Wesley, Redwood City, CA, 1992).
[19] G. B. Whitham, *Linear and Nonlinear Waves* (Wiley, New York, 1974).